Expression of macrophage migration inhibitory factor in footpad skin lesions with diabetic neuropathy

Sun Up Noh[1] iD, Won-Young Lee[1,2], Won-Serk Kim[1,3], Yong-Taek Lee[1,4], and Kyung Jae Yoon[1,4]

Abstract

Background: Diabetic neuropathy originating in distal lower extremities is associated with pain early in the disease course, overwhelming in the feet. However, the pathogenesis of diabetic neuropathy remains unclear. Macrophage migration inhibitory factor has been implicated in the onset of neuropathic pain and the development of diabetes. Objective of this study was to observe pain syndromes elicited in the footpad of diabetic neuropathy rat model and to assess the contributory role of migration inhibitory factor in the pathogenesis of diabetic neuropathy.

Methods: Diabetic neuropathy was made in Sprague Dawley rats by streptozotocin. Pain threshold was evaluated using von Frey monofilaments for 24 weeks. On comparable experiment time after streptozotocin injection, all footpads were prepared for following procedures; glutathione assay, terminal deoxynucleotidyl transferase-mediated biotinylated UTP nick end labeling staining, immunohistochemistry staining, real-time reverse transcription polymerase chain reaction, and Western blot. Additionally, human HaCaT skin keratinocytes were treated with methylglyoxal, transfected with migration inhibitory factor/control small interfering RNA, and prepared for real-time reverse transcription polymerase chain reaction and Western blot.

Results: As compared to sham group, pain threshold was significantly reduced in diabetic neuropathy group, and glutathione was decreased in footpad skin, simultaneously, cell death was increased. Over-expression of migration inhibitory factor, accompanied by low expression of glyoxalase-I and intraepidermal nerve fibers, was shown on the footpad skin lesions of diabetic neuropathy. But, there was no significance in expression of neurotransmitters and inflammatory mediators such as transient receptor potential vanilloid 1, mas-related G protein coupled receptor D, nuclear factor kappa B, tumor necrosis factor-alpha, and interleukin-6 between diabetic neuropathy group and sham group. Intriguingly, small interfering RNA-transfected knockdown of the migration inhibitory factor gene in methylglyoxal-treated skin keratinocytes increased expression of glyoxalase-I and intraepidermal nerve fibers in comparison with control small interfering RNA-transfected cells, which was decreased by induction of methylglyoxal.

Conclusions: Our findings suggest that migration inhibitory factor can aggravate diabetic neuropathy by suppressing glyoxalase-I and intraepidermal nerve fibers on the footpad skin lesions and provoke pain. Taken together, migration inhibitory factor might offer a pharmacological approach to alleviate pain syndromes in diabetic neuropathy.

Keywords

Diabetic neuropathy, macrophage migration inhibitory factor, glyoxalase-I, intraepidermal nerve fibers, footpad skin, pain

Date Received: 26 October 2017; revised: 18 February 2018; accepted: 22 March 2018

[1]Medical Research Institute, Kangbuk Samsung Hospital, Sungkyunkwan University School of Medicine, Republic of Korea
[2]Division of Endocrinology and Metabolism, Department of Internal Medicine, Kangbuk Samsung Hospital, Sungkyunkwan University School of Medicine, Republic of Korea
[3]Department of Dermatology, Kangbuk Samsung Hospital, Sungkyunkwan University School of Medicine, Republic of Korea

[4]Department of Physical and Rehabilitation Medicine, Kangbuk Samsung Hospital, Sungkyunkwan University School of Medicine, Republic of Korea

Corresponding Authors:
Yong-Taek Lee and Kyung Jae Yoon, Department of Physical and Rehabilitation Medicine, Kangbuk Samsung Hospital, Sungkyunkwan University School of Medicine, 29 Saemunan-ro, Jongno-gu, Seoul 110-746, Republic of Korea.
Emails: chocolatebox919@gmail.com; yongtaek1.lee@gmail.com

Introduction

Diabetic neuropathy (DN) originates in the distal lower extremities and is associated with pain early in the disease course, overwhelmingly in the feet.[1,2] The pathogenesis of DN has been described as diabetes-induced hyperglycemia that leads to accumulation of advanced glycation end products (AGEs), thereby damaging intraepidermal nerve fibers (IENF) and provoking pain.[3–5] As AGEs form in the body, the glyoxalase system composed of glyoxalase I (GLO-I) and glyoxalase II is known to detoxify precursors of AGEs such as methylglyoxal (MG) using glutathione (GSH), a physiologically occurring reductant.[6] Accumulating evidence has demonstrated that GLO-I plays a role in protecting against DN.[7,8] For instance, diabetes-induced GLO-I knockdown mice have exaggerated loss of intraepidermal innervation and pain development, compared to wild-type diabetic mice.[8] Moreover, high prevalence of DN has also been observed in individuals with normal glucose tolerance and prediabetes.[9,10] This suggests the need to consider nonglycemic parameters for DN independent of impaired glucose metabolism. However, factors triggering DN remain largely unknown.

Recently, macrophage migration inhibitory factor (MIF) has been implicated in the development and maintenance of diabetes.[11–13] It was first described as a T cell cytokine, named for its ability to cause macrophage arrest in inflammatory exudates. MIF is now recognized as a pro-inflammatory cytokine, and an endocrine hormone such as regulator counteracting anti-inflammatory and immunosuppressive actions of steroids.[14,15] This has also been demonstrated in our previous study using human keratinocytes in vitro.[16] Basal circulating concentrations of MIF are a thousand times higher than other cytokines such as tumor necrosis factor-alpha (TNF-α) and interleukin-6 (IL-6).[17] Some researches have reported that MIF could exaggerate pain responses ascribed to steroids.[18] In addition, MIF can function as oxidoreductase to regulate electron transmission. For instance, it has been shown that MIF can catalyze the reduction of insulin disulfide using physiologically occurring GSH as a reductant.[19]

Since a large number of studies support the pleiotropic function of MIF, the possibility that MIF may initiate or amplify the pain of footpad in DN cannot be excluded. In addition, MIF may correlate with GLO-I and IENF for the onset of pain in DN. However, the role of MIF in DN has not been reported yet.

Therefore, we aimed to observe pain syndromes elicited in the footpad of DN rat model and examine the role of neurotransmitters, metabolic and inflammatory mediators, MIF, GLO-I, and IENF in footpad skin lesions of DN. We then assessed the contributory role of MIF in the pathogenesis of DN by performing small interfering RNA (siRNA)-mediated knockdown of MIF gene or treating with recombinant MIF in human HaCaT keratinocytes.

Materials and methods

Animals

All animal care handling and experimental procedures were carried out in accordance with a protocol approved by the Ethics Committee for Animal Experiments of the Sungkyunkwan University, Kangbuk Samsung Hospital. Male Sprague Dawley rats (200–220 g each, six weeks old, $n = 48$) were used. All rats were housed in a room with 12-h light/dark cycle at $22 \pm 1°C$. They were placed individually in separate cages with ad libitum free access to sufficient food and water in a specific pathogen-free environment.

Induction of diabetes

Experimental DN was induced in male Sprague Dawley rats weighing 250 to 300 g by a single intraperitoneal injection of 70 mg/kg streptozotocin (STZ, Sigma-Aldrich, St. Louis, MO, USA) to achieve maximal induced diabetic ratio and maintain stable and chronic hyperglycemic state. Rats in the sham group were of the same gender and weight. They received intraperitoneal injection of phosphate-buffered saline (PBS). Blood glucose levels and body weight were checked every week following STZ injection. Glucose was measured with a glucose meter (ACCU-CHEK, Roche, Nutley, NJ, USA) using whole blood taken from ventral tail vein. Diabetes was confirmed by persistently elevated blood glucose level greater than 270 mg/dL.

Behavior testing

After diabetes induction, mechanical sensitivity was evaluated weekly using a set of von Frey monofilaments (0.4, 0.6, 1, 2, 4, 6, 8, and 15 g) applied to the plantar surface of the hind paw. Before each behavioral testing session, rats were placed in individual clear acrylic cages (19 × 25 × 14 cm) on a wire mesh screen elevated 70 cm above the table. They were allowed to acclimate for 30 min. The up-down method was used to test mechanical sensitivity. Briefly, beginning with 2-g monofilament, each rat received a single application to the hind paw. Depending on the response of the rat to the previous application, the next smaller filament was used if there was a negative response or the next larger gram filament was used if there was a positive response. A positive response was considered lifting, shaking, or licking of the paw to which the force was applied. Then 50% threshold was calculated for each rat. Group means were determined as previously described in literature.[20]

Baseline behavior testing was measured before diabetes induction.

Processing and preparation of samples

In our study, blood glucose values of 270 mg/dL and over were confirmed at one week after STZ injection. Blood glucose and body weight were recorded every other week until 24 weeks after STZ injection. STZ-induced diabetic rats were also observed for characteristics of painful behaviors from tactile threshold as diabetic duration proceeded until 24 weeks after STZ injection. Footpad thickness was measured using a dial caliper (Kori Seiki MFG, Japan) at 4, 8, 12, and 24 weeks (sacrifice) after diabetes induction. At the end of the experiment, rats were anesthetized by isoflurane and perfused transcardially with saline. All footpads were isolated and excised. Some footpads were immediately frozen in liquid nitrogen and stored at $-80°C$ for performing real-time reverse transcription polymerase chain reaction (RT-PCR) and Western blot. Other footpads were fixed with 10% formalin and embedded in paraffin for terminal deoxynucleotidyl transferase-mediated biotinylated UTP nick end labeling (TUNEL) analysis and immunohistochemistry.

GSH measurement and TUNEL staining

Footpads skin samples were lysed in 0.6% sulfosalicylic acid/0.1% Triton X-100 in phosphate buffer containing 5 mM ethylenediaminetetraacetic acid. Total GSH/oxidized glutathione levels were measured using GSH assay kit (Cayman Chemical Co., Ann Arbor, MI, USA) based on enzymatic recycling method as previously described in literature.[21] Deparaffinized footpads skin sections were stained by TUNEL In Situ Cell Death Detection Kit (Roche Applied Science, Mannheim, Germany) according to the manufacturer's protocol. These sections were incubated in 0.1% sodium citrate containing 0.1% Triton X-100 for 2 min on ice to increase tissue permeability. After rinsing in PBS, 50 μl of TUNEL reaction mixture (calf thymus terminal deoxynucleotidyl transferase and nucleotides) was added to each sample. After incubation at 37°C in the dark for 60 min, these sections were rinsed with PBS and nuclei were stained with 4′, 6-diamidino-2-phenylindole using VECTARSHIELD mounting medium (Vector Laboratories, Inc., Burlingame, CA, USA). Sections were then covered with coverslips and observed under an Olympus BX51 microscope (Olympus Optical Co., Tokyo, Japan).

Immunohistochemistry staining

Footpads were fixed with 10% formalin, embedded in paraffin, and sectioned (4 μm in thickness) onto silane-coated micro slide (Muto-glass, Tokyo, Japan). These de-paraffinized skin sections were then subjected to immunohistochemistry staining. Briefly, sections were rinsed with distilled water. Endogenous peroxidase activity was blocked with 3% hydrogen peroxide solution diluted with methanol. After rinsing with PBS, sections were incubated with 0.01 M citrate buffer (pH 6) at 100°C for 15 min followed by incubation at room temperature for 40 min. Non-specific antigen-antibody reactions were then inhibited by 1-h treatment with 2.5% normal horse serum (Vector Laboratories). These sections were reacted with primary antibodies such as purified rabbit polyclonal antibodies against anti-rat MIF (1:50), IENF (1:50), and GLO-I (1:100) (Santa Cruz Biotechnology, Inc., Delaware, CA, USA) overnight at 4°C. After rinsing with PBS, they were reacted with secondary antibody (horseradish peroxidase micro-polymer anti-rabbit IgG, Vector Laboratories) at room temperature for 1 h. For chromogen reactions, Vector® NovaRED™ substrate kit (Vector Laboratories) was used, including reactions with reagent 1, 2, and 3, and hydrogen peroxide at room temperature within 2 min. After chromogen reactions, these sections were rinsed with distilled water and PBS. They were then counterstained with hematoxylin (Vector Laboratories). Rinsed sections were made transparent with xylene treatment via dehydration. They were then covered with permount and examined by light microscope to assess histological changes.

Cell culture, treatment, and MIF siRNA transfection

Immortalized HaCaT cells (No. 300493; Cell Lines Service, Eppelheim, Germany) derived from spontaneous transformation of human adult keratinocytes were provided by Professor Kim (Sungkyunkwan University College of Medicine, Seoul, Republic of Korea). Cells were cultured in Dulbecco's modified Eagle medium (Gibco, Rockville, MD, USA) supplemented with 10% fetal bovine serum (Gibco) and 1% penicillin/streptomycin (Gibco) in a humidified atmosphere of 95% air and 5% CO_2 at 37°C. Cell culture medium was refreshed until cells reached 80% confluency. Cells were then passaged and harvested using TrypLE™ express (Gibco). These cells were then seeded onto six-well culture plates (Nunc, Naperville, IL, USA) at a density of 2×10^5 cells per well. When cells reached 80% confluency, various concentrations of MG (100, 200, or 400 μm; Sigma-Aldrich) were added to each well followed by incubation for 12 h. In some experiments, 400 μm MG was added to cells treated with recombinant human MIF (rh-MIF) (1 or 10 ng/ml; R&D systems, Inc. Minneapolis, MN, USA). Cells were then transfected with MIF siRNA/control siRNA (Santa Cruz Biotechnology) using Lipofectamine RNAiMAX reagent (Invitrogen Life

Technologies, Carlsbad, CA, USA) according to the manufacturer's protocol and incubated for 24 h before further manipulation.

RNA isolation and real-time RT-PCR

Total RNAs were extracted from tissues and cells using TRIzol reagent (Invitrogen) according to the manufacturer's protocol. An equal amount of 10 μg total RNA was obtained from each sample and reverse-transcribed into cDNA using oligo(dT)15 primers and M-MLV reverse transcriptase (Promega, Madison, WI, USA). These cDNAs were then subjected to real-time RT-PCR (LightCycler 480 system; Roche Diagnostics, Indianapolis, IN, USA) using 2x SYBR Green master mix kit (Roche Diagnostics). The following gene-specific primer pairs were used: MIF (forward, 5′-CCCAGAA CCGCAACTACAGCAA-3′; reverse, 5′-CGTTGGC TGCGTTCATGTCGTAAT-3′), GLO-I (forward, 5′-GAAGATGACGAGACGCAGAGTTAC-3′; reverse, 5′-CAGGATCTTGAACGAACGCCAGAC-3′), IENF (forward, 5′-AGTGGCTCTCTGCAAAGCAG-3′; reverse, 5′-GGCAGTAGAACGCAAGAAGA-3′), receptor for advanced glycation end product (RAGE) (forward, 5′-GGAAGGACTGAAGCTTGGAAGG-3′; reverse, 5′-TCCGATAGCTGGAAGGAGGAGT-3′), transient receptor potential vanilloid 1 (TRPV1) (forward, 5′-GACATGCCACCCAGCAGG-3′; reverse, 5′-TCAA TTCCCACACACCTCCC-3′), mas-related G protein coupled receptor D (MRGPRD) (forward, 5′-CTGTC GAGTTTCCACAGGTTCC-3′; reverse, 5′-TTGCGCA GAGGTACGGTTCC-3′), calcitonin gene-related peptide (CGRP) (forward, 5′-CTGTCGAGTTTC CACAGGTTCC-3′; reverse, 5′-TTGCGCAGAGGTA CGGTTCC-3′), nuclear factor kappa B (NF-kB) (forward, 5′-GGCAGCACTCCTTATCAA-3′; reverse, 5′-GGTGTCGTCCCATCGTAG-3′), TNF-α (forward, 5′-CCCACGTCGTAGCAAACCACCA-3′; reverse, 5′-CCATTGGCCAGGAGGGCGTTG-3′), and IL-6 (forward, 5′-CCTGGAGTTTGTGAAGAACAACT-3′; reverse, 5′-GGAAGTTGGGGTAGGAAGGA-3′). Primer sequences specificity was confirmed by performing BLAST analysis for similar sequences against known sequence databases. PCR product was measured using SYBR Green fluorescence collected on a LightCycler 480 system. Melting point analyses were performed for each reaction to confirm single amplified products. △△Ct method was used to analyze gene expression levels normalized against β-actin expression. All experiments were performed in duplicate.

Protein preparation and Western blot analysis

Tissues and cells were lysed in radioimmuno precipitation assay buffer (Pierce, Rockford, IL, USA) with protease inhibitor cocktail (Roche). Cell lysates were centrifuged at 10,000 r/min for 7 min at 4°C, and supernatants were obtained. Protein content was quantified with a standard bicinchoninic acid protein assay reagent (Pierce). Equal amounts of protein (20 μg) were separated by electrophoresis on 4% to 12% bis-tris gel and then transferred to polyvinylidenedifluoride membrane using iBlot Transfer Stack (Invitrogen). Blots were stained with Ponseau S (Amrecso, Fountain parkway, Solon, OH, USA) to visualize protein bands and ensure equal protein loading and uniform transfer. Blots were washed and blocked with 5% nondried skim milk in Tris buffered saline/Tween20 for 1 h. Blots were probed overnight at 4°C with antibodies. Rabbit polyclonal antibody against MIF (1:200, Santa Cruz) and mouse monoclonal antibodies against IENF (1:200), GLO-I (1:1000) (Abcam, Cambridge, MA, USA) or β-actin (1:200, Santa Cruz) were used in this study. These blots were then incubated with corresponding horseradish peroxidase conjugated anti-rabbit (1:5000) or anti-mouse (1:2000) immunoglobulin G antibodies (Santa Cruz). Immunoreactive proteins were visualized using an enhanced chemiluminescence system (Amersham, Piscataway, NJ, USA). Relative density was measured using ImageJ software (NIH, Bethesda, MD, USA). Results are representatives of five independent experiments.

Statistical analysis

All data are expressed as mean $\pm SE$. PASW statistics 18.0 (SPSS, Chicago, USA) was used for all statistical analyses. Differences among groups were determined by Student's t test with Bonferroni correction for comparison between two groups or one-way analysis of variance following Tukey post hoc test. Statistical significance is presented as $P < 0.05$, $P < 0.01$, or $P < 0.005$.

Results

STZ-induced diabetes

To confirm successful induction of diabetes, we measured blood glucose levels and body weights. Blood glucose levels of rats in the sham group remained below 270 mg/dL. They were increased rapidly in SD rats within one week after STZ intraperitoneal injection. Their hyperglycemic states maintained progressively until the 24th week (sham: 128.8 ± 16.1 vs. DN: 508.7 ± 60.5 mg/dl, $P < 0.005$) in the DN group (Figure 1(a)). Compared to body weight of rats in the sham group, body weight in STZ-induced DN group was decreased continuously until the 24th week (sham: 638.4 ± 63.8 vs. DN: 384.5 ± 58.1 g, $P < 0.005$). Rats in the sham group kept growing. Their body weights exceeded 500 g
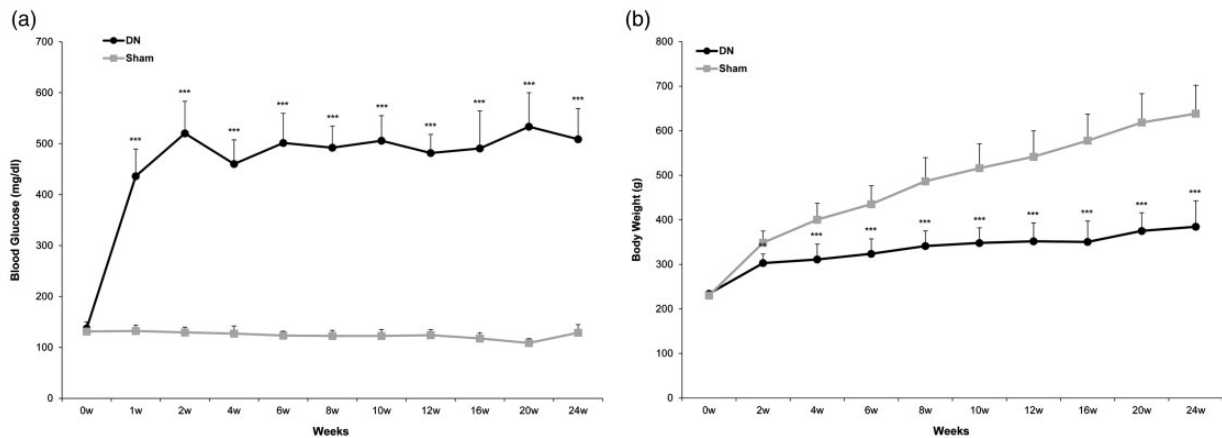
(a)

(b)

Figure 1. (a) Blood glucose level and (b) body weight changes after streptozotocin (STZ) or saline treatment in Sprague Dawley rats. Experimental diabetic neuropathy (DN) was induced in male Sprague Dawley rats weighing 250 to 300g by a single intraperitoneal injection of 70 mg/kg STZ to achieve a maximal induced diabetic ratio and maintain a stable and chronic hyperglycemic state. Diabetes was confirmed by a persistently elevated blood glucose level greater than 270 mg/dL. Blood glucose level and body weight were checked for 24 weeks. All values are expressed as mean $\pm$ standard deviation (SD) ($n=$ 6 per group). $^{**}P<0.01$, $^{***}P<0.005$ compared to those in the sham group.

(Figure 1(b)). DN rats also displayed other characteristic symptoms of type I diabetes, including polyuria and polydipsia.

Behavioral sensitivity to mechanical stimuli

To evaluate pain-related sensory responses after induction of diabetes, mechanical sensitivity was evaluated directly by hind paw withdrawal using von Frey monofilaments. The 50% withdrawal thresholds of DN rats at six and eight weeks after STZ injection were 14.7 ± 1.6 g and 7.28 ± 3.0 g, while those of sham rats at six and eight weeks after saline injection were 15.1 ± 1.6 g and 14.8 ± 0.4 g, respectively. Compared to that of the sham group, pain threshold was lower by approximately two fold in the DN group as early as the eighth week after the induction of diabetes ($P < 0.005$, Figure 2). After that, differences in threshold between the two groups became more prominent. After 24 weeks of diabetes, DN rats had mechanical thresholds of 1.6 ± 1.1 g, while sham rats had thresholds of 14.4 ± 1.4 g. The pain threshold in the DN group was >nine fold lower compared to that in the sham group at the 24th week ($P < 0.005$, Figure 2).

Relationship between oxidative stress and apoptotic cell death in footpad skin of DN

To histologically evaluate oxidative stress and damage on footpad skin lesions in the DN group, we measured GSH levels and apoptosis for specimens of footpads obtained from SD rats. DN group showed a marked decrease in GSH level in footpad skin compared to the
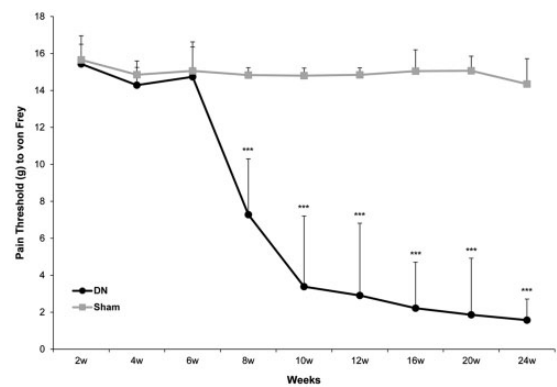

Figure 2. Behavior phenotype of mechanical sensitivity in a diabetic neuropathy (DN) rat model. Mechanical threshold was evaluated weekly using a set of von Frey monofilaments (0.4, 0.6, 1, 2, 4, 6, 8, and 15 g) applied to the plantar surface of the hind paw. Beginning with 2-g monofilament, the next smaller filament was used if there was a negative response or the next larger gram filament was used if there was a positive response. All data are expressed as mean $\pm$ standard deviation (SD) ($n=$ 6 per group). $^{***}P<0.005$ compared to that in the sham group.

sham group (8th week $= 6.4 \pm 1.8$ vs. 79.0 ± 21.6, $P < 0.05$; 12th week $= 6.4 \pm 5.4$ vs. 110.8 ± 1.8, $P < 0.005$; 24th week $= 3.8 \pm 1.8$ vs. 68.8 ± 7.2 nmol min^{-1} ml^{-1}, $P < 0.01$; Figure 3(a)). Thickening of footpads in the DN group was first observed in the fourth week. It was definitely decreased in the 12th week (3.1 ± 0.2 vs. 4.0 ± 0.1 mm, $P < 0.005$) compared to that in the sham group. It was then steadily decreased until the 24th week (3.4 ± 0.3 vs. 4.1 ± 0.1 mm, $P < 0.005$) compared to that in the sham group (Figure 3(b)). We also evaluated apoptotic cell death by using TUNEL staining. After four weeks of STZ injection, there was no
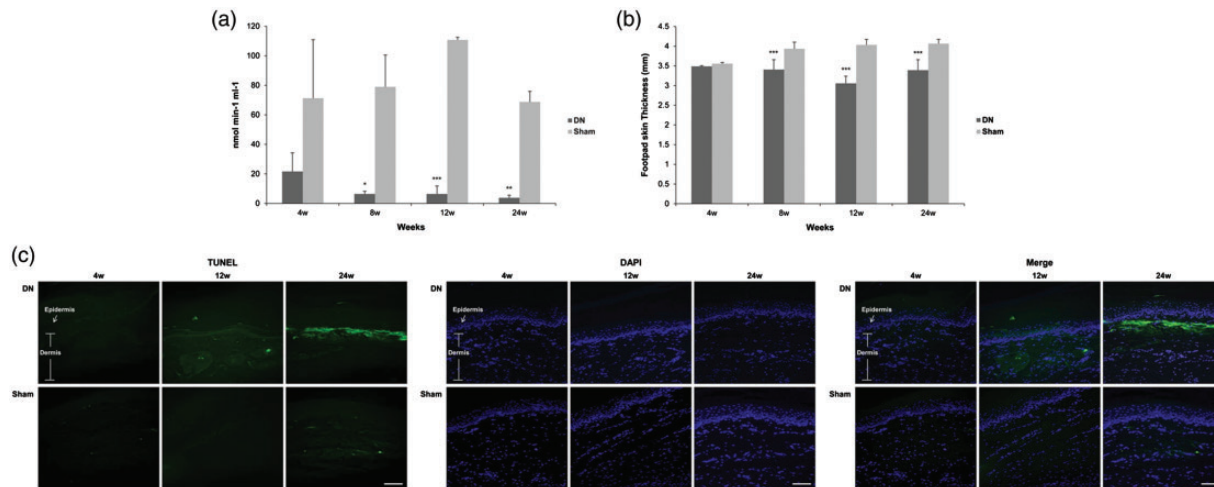
Figure 3. Changes of (a) glutathione (GSH) level, (b) footpad skin thickness, and (c) terminal deoxynucleotidyl transferase biotin-dUTP nick-end labeling (TUNEL, green), 4′, 6-diamidino-2-phenylindole (blue) staining in footpad skin lesions from a diabetic neuropathy rat model. Footpad thickness was measured using a dial caliper. Footpad skin tissues were excised, and GSH levels were measured using GSH assay kit. Some footpads were fixed in 10% formalin and embedded in paraffin. De-paraffinized sections (4 μm thick) were stained for TUNEL assay. Values are shown as mean ± standard deviation (SD) (n= 6 per group). Sections were observed with magnification of ×200, scale bar (white) = 60 μm. $^*P < 0.05$, $^{**}P < 0.01$, $^{***}P < 0.005$ compared to that in the sham group.

Table 1. Expression mRNA levels of neurotransmitter and metabolic or inflammatory mediators in footpad skin lesions after 12 weeks of diabetic neuropathy.

	MIF	GLO-I	IENF	RAGE	TRPV1	MRGPRD	CGRP	NF kB	TNF-α	IL-6
DN	11.32±0.66***	0.34±0.01***	0.25±0.01***	1.16±0.09*	0.84±0.09	1.19±0.05	1.12±0.02	7.16±1.70	0.66±0.16	1.46±0.93
Sham	1.04±0.06	2.19±0.17	1.55±0.03	0.61±0.00	1.00±0.10	1.00±0.05	1.02±0.10	5.73±0.28	0.53±0.04	0.72±0.50

MIF: macrophage migration inhibitory factor; GLO-I: glyoxalase-I; IENF: intraepidermal nerve fibers; RAGE: receptor for advanced glycation end product; TRPV1: transient receptor potential vanilloid 1; MRGPRD: mas-related G protein coupled receptor D; CGRP: calcitonin gene-related peptide; NF-kB: nuclear factor kappa B; TNF-α: tumor necrosis factor-alpha; IL-6: interleukin-6.

mRNA relative fold increase (mean ± SE). Real-time polymerase chain reaction was performed with a SYBR Green assay system. Relative gene expression levels normalized to that of β-actin was determined with $2^{-\Delta\Delta CT}$ method.

$^*P < 0.05$, $^{***}P < 0.005$ compared to that in the sham group.

TUNEL-positive cell in DN skin. In the 12th and 24th week after STZ injection, the DN group exhibited more TUNEL-positive cells, especially in intraepidermal cells compared to the sham group (Figure 3(c)). These results showed that enhanced oxidative stress facilitated skin thinning which in turn, led to apoptosis of DN footpad skin.

Pain-related indicators in footpad skin lesions of DN

To determine whether neurotransmitters and metabolic or inflammatory mediators might play a role in activating sensory nerve to provoke pain sensation and inflammation and aggravate symptoms in the feet of DN, we performed real-time RT-PCR to determine expression levels of MIF, GLO-I, IENF, RAGE, TRPV1, MRGPRD, CGRP, NF-kB, TNF-α, and IL-6 in

footpad skin after 12 weeks of diabetes. As shown in Table 1, mRNA levels of MIF were sharply higher in the DN group ($P < 0.005$) compared to that in the sham group. Conversely, mRNA levels of GLO-I and IENF were significantly lower in the DN group ($P < 0.005$) compared to those in the sham group. RAGE mRNA expression levels were slightly but significantly up-regulated in the DN group ($P < 0.05$) compared to that in the sham group. On the other hand, there was no significant difference in mRNA expression levels of TRPV1, MRGPRD, CGRP, NF-kB, TNF-α, or IL-6 between the two groups. These results indicated that a few metabolic mediators such as MIF, GLO-I, IENF, and RAGE but not transmitters or inflammatory cytokines such as TRPV1, MRGPRD, CGRP, NF-kB, TNF-α, and IL-6 were more involved in the pain symptoms of DN-like footpad skin lesions.

Real-time RT-PCR results for expressions of MIF, GLO-I, and IENF at different time points in footpad skin lesions of DN

To investigate more concretely the expression of MIF, IENF, and GLO-I related to symptoms in the feet of DN, levels of mRNA transcripts of MIF, IENF, and GLO-I at different time points in footpad skin samples were quantitatively measured by real-time RT-PCR. As shown in Figure 4(a), mRNA expression levels of MIF were significantly up-regulated in the DN group at 8th (8.78 ± 0.99 vs. 2.00 ± 0.12, $P < 0.01$), 12th (11.32 ± 0.67 vs. 1.04 ± 0.07, $P < 0.005$), and 24th week (17.51 ± 0.43 vs. 1.29 ± 0.04, $P < 0.005$) after STZ injection compared to those in the sham group. Remarkably, the maximal expression of MIF mRNA at 24th week after STZ injection was >13 fold compared to that in the sham group. In contrast, mRNA expression levels of GLO-I were significantly decreased in the DN group at 8th (0.37 ± 0.02 vs. 1.87 ± 0.08, $P < 0.005$), 12th (0.34 ± 0.02 vs. 2.20 ± 0.17, $P < 0.005$), and 24th week (0.46 ± 0.04 vs. 2.35 ± 0.16, $P < 0.005$) after STZ injection compared to those in the sham group (Figure 4 (b)). IENF mRNA expression levels were also significantly down-regulated in the DN group at 8th (0.49 ± 0.05 vs. 1.03 ± 0.13, $P < 0.05$), 12th (0.26 ± 0.01 vs. 1.55 ± 0.04, $P < 0.005$), and 24th week (0.16 ± 0.00 vs. 1.32 ± 0.08, $P < 0.005$) after STZ injection compared to those in the sham group (Figure 4(c)). There was no significant difference in MIF, GLO-I, or IENF mRNA expression at fourth week after STZ injection between the two groups. These results showed that as mRNA levels of MIF were increased, those of GLO-I and IENF were own-regulated in DN-like footpad skin lesions.
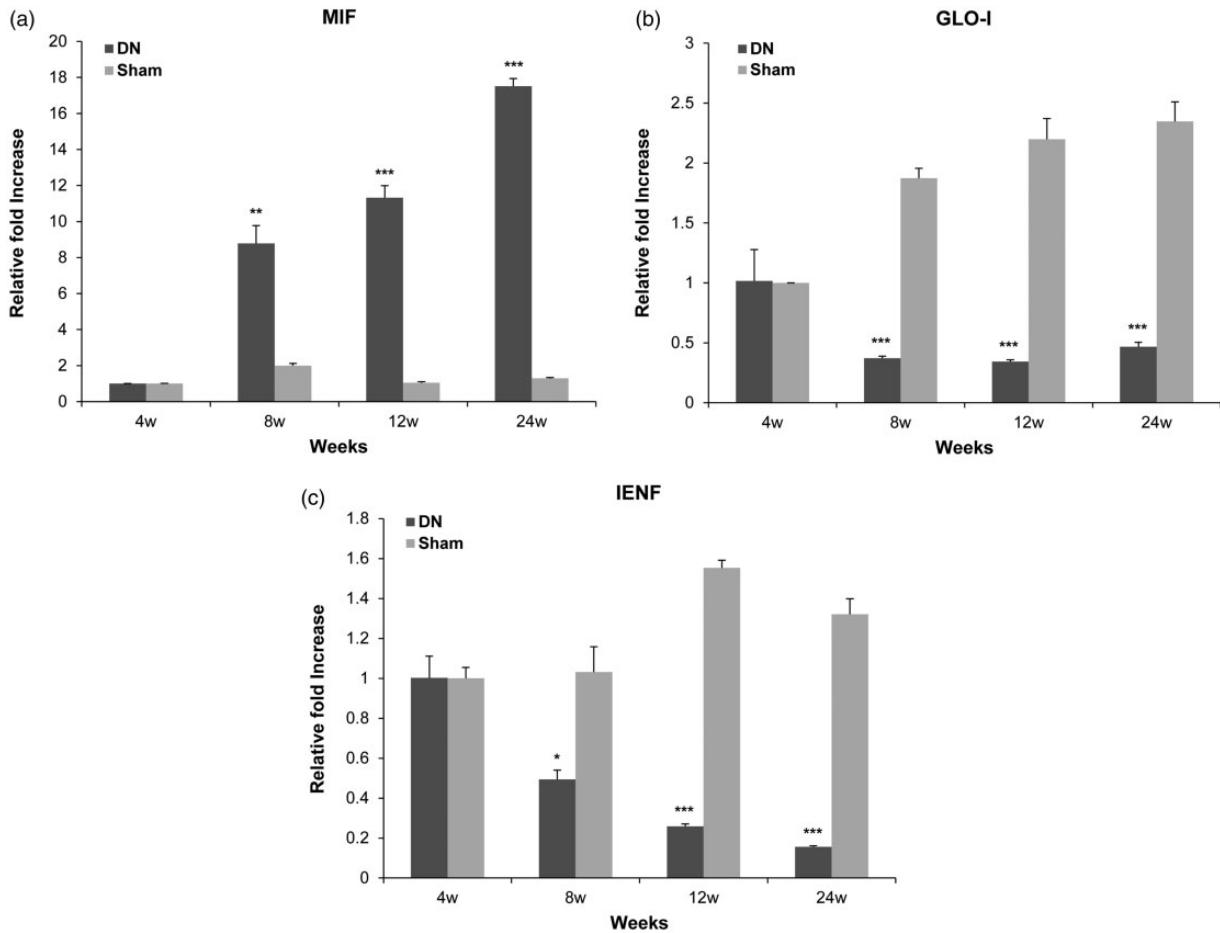

Figure 4. Expressions levels of macrophage migration inhibitory factor (MIF), glyoxalase I (GLO-I), and intraepidermal nerve fibers (IENF) mRNAs in footpad skin lesions in a diabetic neuropathy (DN) rat model. Total RNA (10 μg) obtained from each footpad tissue sample was reverse transcribed into cDNA. Real-time polymerase chain reaction was performed with a SYBR Green assay system. Relative gene expression levels normalized to that of β-actin was determined with $2^{-\Delta\Delta CT}$ method. All columnar values are expressed as mean $\pm$ standard deviation (SD) ($n=$ 6 per group). $^{*}P<0.05$, $^{**}P<0.01$, $^{***}P<0.005$ compared to that in the sham group.

Western blot analysis for expressions of MIF, GLO-I, and IENF in footpad skin lesions of DN

To confirm expression levels of MIF, IENF, and GLO-I in footpad skin lesions in the DN group, Western blot analysis was performed. As shown in Figure 5(a), protein levels of MIF were significantly increased in the DN group at 12th (8.70 ± 0.39 vs. 4.97 ± 0.22, $P < 0.001$) and 24th week (12.38 ± 0.70 vs. 5.13 ± 0.26, $P < 0.005$) after STZ injection compared to those in the sham group (Figure 5(b)). There was no significant difference in MIF protein expression at fourth or eighth week after STZ injection between the two groups. However, GLO-I protein expression levels were significantly decreased in the DN group at 8th (11.63 ± 0.94 vs. 18.79 ± 0.68, $P < 0.05$), 12th (8.44 ± 0.22 vs. 16.27 ± 0.84, $P < 0.01$), and 24th week (4.43 ± 0.19 vs. 16.44 ± 1.90, $P < 0.01$) after STZ injection compared to those in the sham group (Figure 5(c)). Likewise, IENF protein expression levels were significantly down-regulated in the DN group

at 8th (13.72 ± 0.97 vs. 19.39 ± 0.88, $P < 0.05$), 12th (12.80 ± 0.09 vs. 15.15 ± 0.72, $P < 0.05$), and 24th week (10.99 ± 0.78 vs. 18.96 ± 0.03, $P < 0.005$) after STZ injection compared to those in the sham group (Figure 5(d)). There was no significant difference in GLO-I or IENF protein expression at fourth week after STZ injection between the two groups. These results indicated that increased expression of MIF accompanied by low expression of GLO-I was involved in reduced IENF in diabetic footpad skin.

Immunohistochemistry results for expressions of MIF, GLO-I, and IENF in footpad skin lesions of DN

To further assess their localization in footpad skin lesions in the DN group, immunohistochemistry staining was performed for MIF, IENF, and GLO-I. As shown in Figure 6(a), MIF was strongly over-expressed until the 24th week after STZ injection throughout the whole epidermal layer on footpad skin lesions in the
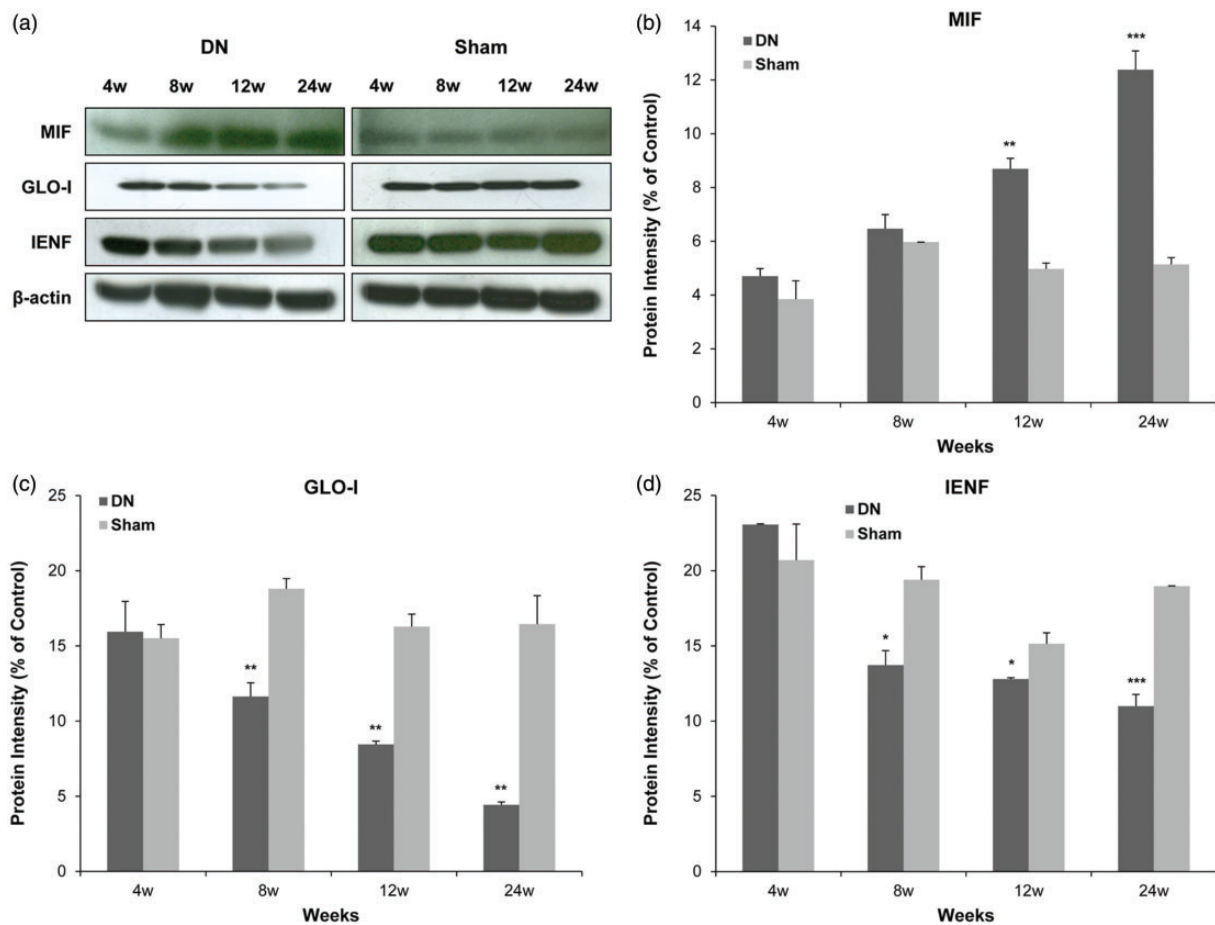

Figure 5. Protein expression levels of macrophage migration inhibitory factor (MIF), glyoxalase I (GLO-I), and intraepidermal nerve fibers (IENF) in footpad skin lesions in a diabetic neuropathy (DN) rat model. Protein (20 μg) was obtained from each footpad tissue sample. Protein levels were examined by Western blot. As a control for Western blot analysis, the level of β-actin was determined using an antibody against β-actin. All columnar values are expressed as mean ± standard deviation (SD) ($n = 6$ per group). $^{*}P < 0.05$, $^{**}P < 0.01$, $^{***}P < 0.005$ compared to that in the sham group.
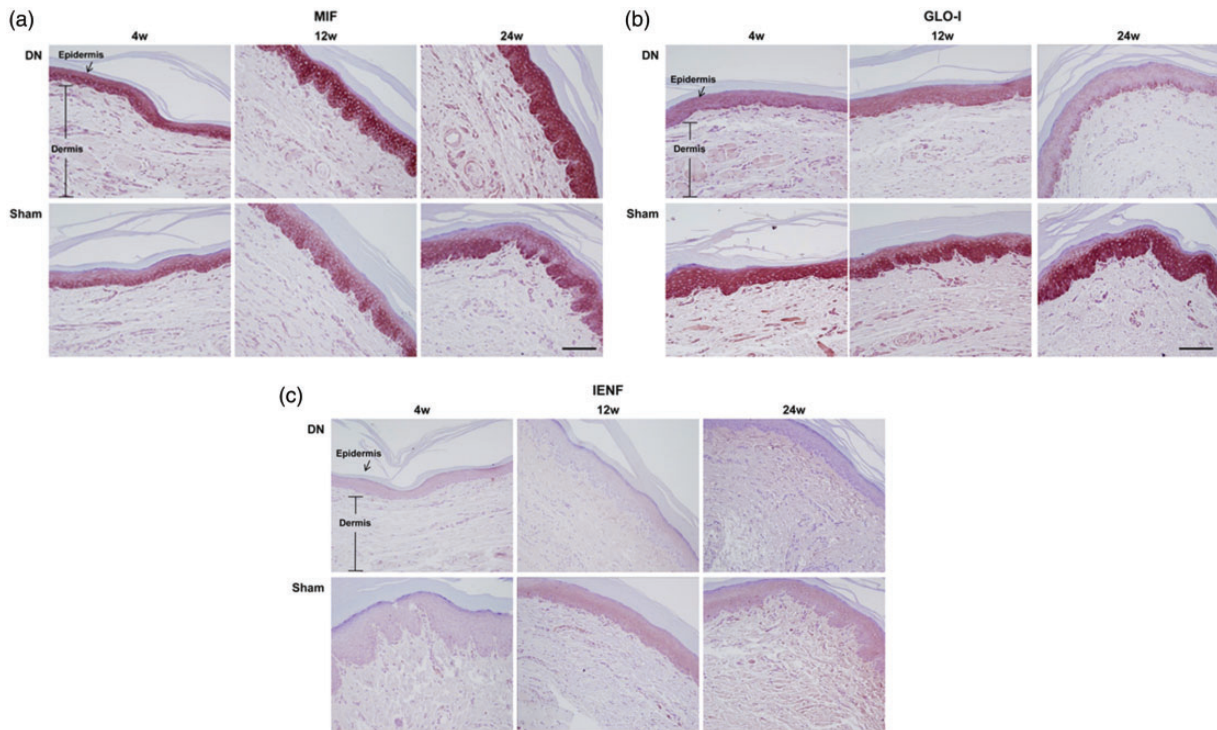
Figure 6. Histological expressions of macrophage migration inhibitory factor (MIF), glyoxalase I (GLO-I), and intraepidermal nerve fibers (IENF) in footpad skin lesions in a diabetic neuropathy (DN) rat model. Footpads were fixed in 10% formalin and embedded in paraffin. De-paraffinized sections (4 μm thick) were prepared for immunohistochemistry staining. They were examined under a light microscope to assess histological changes. Sections were observed at magnification of ×200. Scale bar (black) = 60 μm. A representative picture from three independent immunohistochemistry staining experiments is shown.

DN group compared to that in the sham group, in which MIF expression was mostly limited to the basal layer of the epidermis. On the other hand, both GLO-I and IENF showed progressively weak staining until the 24th week after STZ injection in the intraepidermal layer of skin lesions in the DN group in comparison with those of the sham group (Figure 6(b) and (c)). Especially, MIF was mainly stained in the basal layer of the epidermis in the sham group, showing immuno-histochemical colocalization with GLO-I. However, MIF was overexpressed on the entire layer of the epidermis at large while GLO-I was faintly stained on the basal layer of the epidermis in the DN group at 24 weeks after STZ injection.

MG treatment in skin kertatinocytes as an in vitro model of footpad skin with DN

To examine correlations in expression of MIF, GLO-I, and IENF in footpad skin lesions of DN rats, we designed an in vitro model using cultured human skin keratinocytes, HaCaT cells. HaCaT keratinocytes were treated with MG at different concentrations (100, 200, and 400 μm) to mimic hyperglycemic status. After 12-h treatment with MG, levels of mRNA transcripts of MIF, IENF, and GLO-I were quantitatively measured by real-time RT-PCR. As shown in Figure 7(a), levels of MIF mRNA were significantly up-regulated in MG-treated groups (100 μm: 22.24 ± 0.43, $P < 0.005$; 200 μm: 39.84 ± 2.53, $P < 0.005$; and 400 μm: 120.29 ± 4.12, $P < 0.005$) compared to those in the negative control (1.00 ± 0.00). The maximal level of MIF mRNA in 400 μm MG-treated group was >120 fold compared to that in the negative control. Conversely, GLO-I mRNA levels were significantly down-regulated in MG-treated groups (100 μm: 0.32 ± 0.11, $P < 0.05$; 200 μm: 0.46 ± 0.01, $P < 0.01$; and 400 μm: 0.55 ± 0.00, $P < 0.005$) compared to those in the negative control (1.00 ± 0.00) (Figure 7(b)). IENF mRNA levels were also significantly decreased in MG-treated groups (100 μm: 0.48 ± 0.07, $P < 0.01$; 200 μm: 0.53 ± 0.05, $P < 0.01$; and 400 μm: 0.59 ± 0.04, $P < 0.01$) compared to those in the negative control (1.00 ± 0.00) (Figure 7(c)). Additionally, we performed Western blot analysis to determine protein levels of MIF, GLO-I, and IENF. As shown in Figure 7(d), MIF protein expression levels were significantly increased in MG-treated groups (100 μm: 10.75 ± 0.04, $P < 0.005$; 200 μm: 13.77 ± 1.21, $P < 0.05$; and 400 μm: 18.57 ± 2.74, $P < 0.05$) compared to those in the negative control (7.77 ± 0.11) (Figure 7(e)). In contrast, expression levels of GLO-I protein were significantly decreased
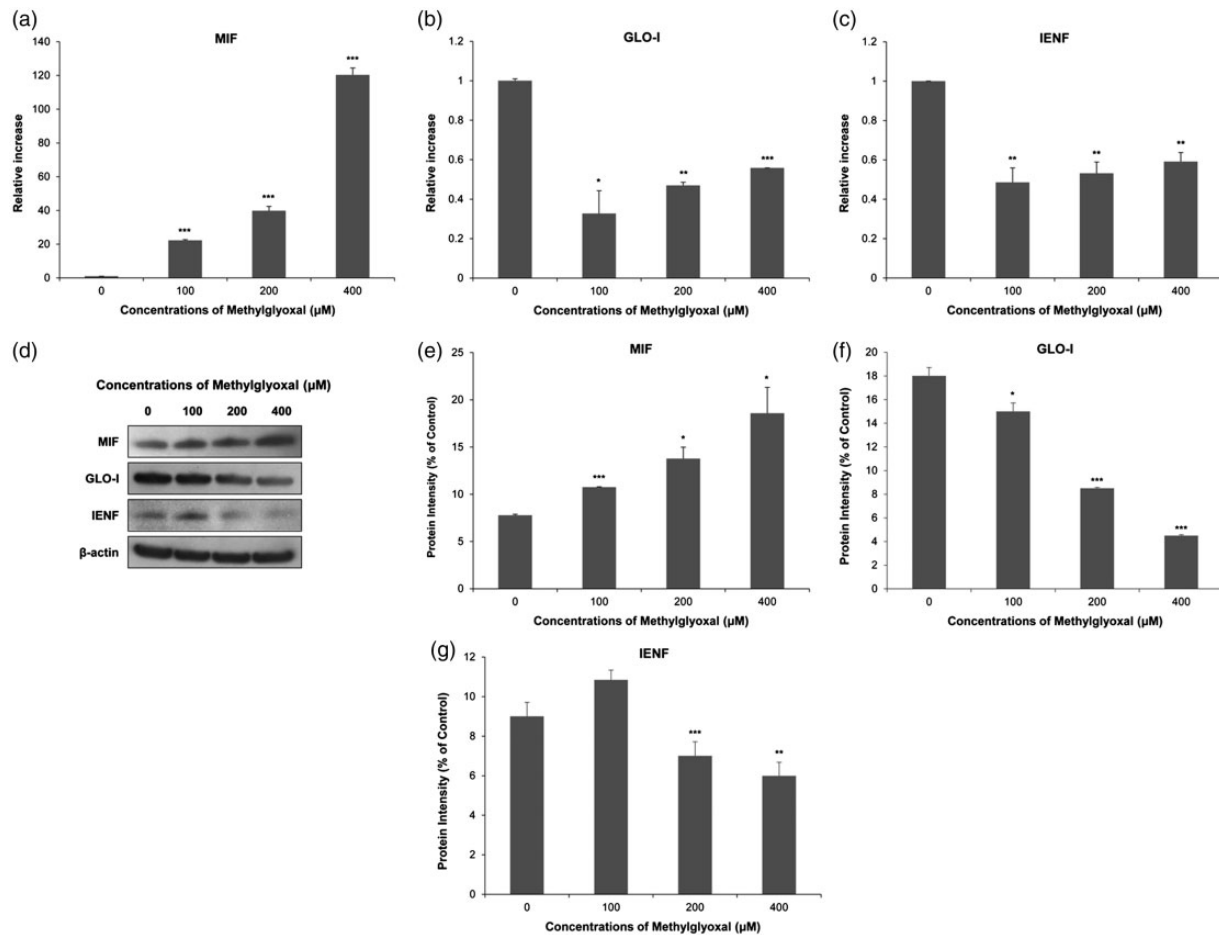
Figure 7. Macrophage migration inhibitory factor (MIF), glyoxalase I (GLO-I), and intraepidermal nerve fibers (IENF) expression level changes in human HaCaT keratinocytes after being exposed to various concentrations of methylglyoxal (MG). Expression levels of MIF, GLO-I, and IENF mRNAs and proteins were measured by real-time reverse transcription polymerase chain reaction (a) to (c) and Western blot (d) to (g), respectively. Real-time PCR analysis was performed with a SYBR Green assay system. Relative gene expression level normalized to β-actin was calculated with $2^{-\triangle\triangle CT}$ method. As a control for Western blot analysis, the level of β-actin was determined using an antibody against β-actin. All results are presented as mean ± SD of three independent experiments. $^{*}P< 0.05$, $^{**}P<0.01$, $^{***}P<0.005$ compared to that in the negative control group.

in MG-treated groups (100 μm: 15.00 ± 0.70, $P \leq 0.05$; 200 μm: 8.49 ± 0.07, $P \leq 0.005$; and 400 μm: 4.49 ± 0.07, $P \leq 0.005$) compared to those in the negative control (17.99 ± 0.70) (Figure 7(f)). IENF protein levels were also significantly decreased in MG-treated groups (200 μm: 7.00 ± 0.71, $P \leq 0.005$; 400 μm: 5.99 ± 0.69, $P \leq 0.01$) compared to those in the negative control (9.00 ± 0.70) (Figure 7(g)). Therefore, we used 400 μm of MG to treat cells as an in vitro model of footpad skin with DN.

MIF capability to drive suppression of GLO-I and IENF under hyperglycemic conditions

To explore whether MIF might contribute to the reduction of GLO-I and IENF on MG-induced hyperglycemic condition in skin keratinocytes, we measured its ability to alter expression of GLO-I and IENF using rh-MIF at

different concentrations. As shown in Figure 8(b) and (c), mRNA levels of GLO-I (0.009 ± 0.000, $P < 0.005$) and IENF (0.080 ± 0.005, $P < 0.005$) were sharply and significantly down-regulated in the group treated with $1 \, \text{ng} \, \text{mL}^{-1}$ rh-MIF compared to those in the vehicle control-treated group (GLO-I: 1.002 ± 0.093; IENF: 1.000 ± 0.000). In the group treated with $10 \, \text{ng} \, \text{mL}^{-1}$ rh-MIF, mRNA levels of GLO-I (0.004 ± 0.000, $P < 0.005$) and IENF (0.000 ± 0.000, $P < 0.005$) were also sharply and significantly down-regulated compared to those in the vehicle control-treated group (GLO-I: 1.002 ± 0.093; IENF: 1.000 ± 0.000). As shown in Figure 8(d), protein levels of GLO-I (2.54 ± 0.09, $P < 0.005$) and IENF (3.79 ± 0.72, $P < 0.05$) were significantly down-regulated in the group treated with $1 \, \text{ng} \, \text{mL}^{-1}$ rh-MIF compared to those in the vehicle control-treated group (GLO-I: 3.72 ± 0.02; IENF: 6.20
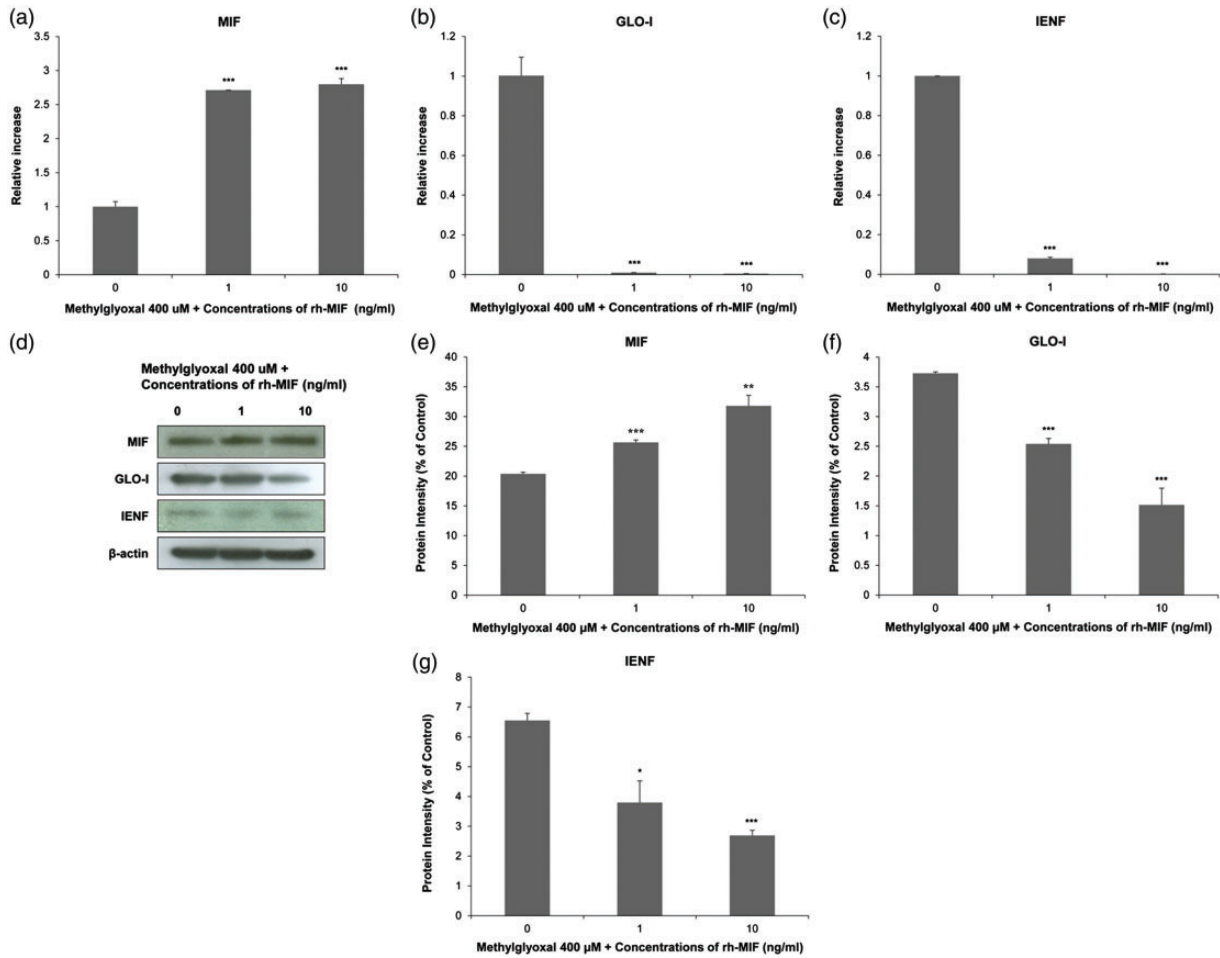
Figure 8. Macrophage migration inhibitory factor (MIF), glyoxalase I (GLO-I), and intraepidermal nerve fibers (IENF) expression level changes in human HaCaT keratinocytes after being exposed to recombinant human (rh)-MIF in the presence of 400 μm MG. Expression levels of MIF, GLO-I, and IENF mRNAs and proteins were measured by real-time reverse transcription polymerase chain reaction (a) to (c) and Western blot (d) to (g), respectively. Real-time PCR analysis was performed with a SYBR Green assay system. Relative gene expression level normalized to β-actin was calculated with $2^{-\triangle\triangle CT}$ method. As a control for Western blot analysis, the level of β-actin was determined using an antibody against β-actin. All results are presented as mean $\pm$ SD of three independent experiments. $^{*}P<0.05$, $^{**}P<0.01$, $^{***}P<0.005$ compared to that in the negative control group.

± 0.72). Protein levels of GLO-I (1.51 ± 0.28, $P < 0.005$) and IENF (3.32 ± 0.72, $P < 0.005$) were also significantly down-regulated in the group treated with $10\,ng\,mL^{-1}$ rh-MIF as compared with those in the vehicle control-treated group (GLO-I: 3.72 ± 0.02; IENF: 6.20 ± 0.72) (Figure 8(f) and (g)). These changes were more pronounced with higher concentrations of rh-MIF. Our results suggest that MIF is capable of reducing GLO-I and IENF levels under diabetic conditions.

MIF efficiency to control deletion of GLO-I and IENF under hyperglycemic conditions

To assess whether MIF deficiency could recover the loss of GLO-I and IENF under hyperglycemic status of skin keratinocytes, we examined expression levels of GLO-I and IENF after transfection with MIF siRNA. Interestingly, mRNA expression levels of GLO-I were significantly increased from 76.37 ± 0.74 to 89.88 ± 0.44 in hyperglycemic keratinocytes treated with 400 μm MG and transfected with MIF siRNA in comparison with control siRNA-transfected cells ($P < 0.005$, Figure 9 (b)). IENF mRNA expression levels were also sharply and significantly up-regulated from 4.30 ± 0.02 to 126.67 ± 0.00 under hyperglycemic conditions after transfection with MIF siRNA compared to those in cells transfected with control siRNA ($P < 0.005$, Figure 9(c)). Likewise, protein levels of GLO-I and IENF were significantly increased ($\geq$by two fold) in the hyperglycemic skin keratinocytes transfected with MIF siRNA in comparison with those in control siRNA-transfected cells ($P < 0.01$ Figure 9(f) and (g)). These results indicate
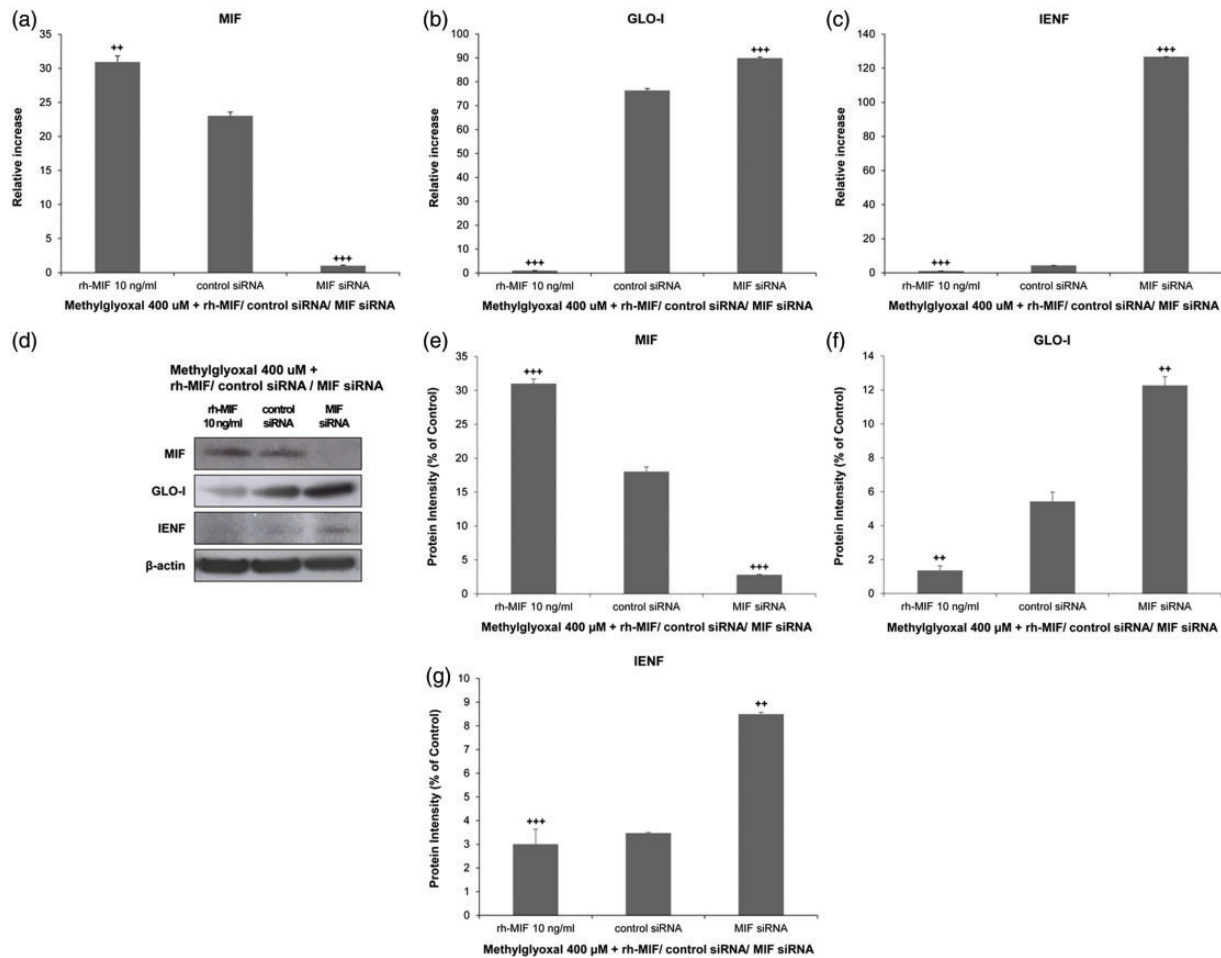
Figure 9. Effects of macrophage migration inhibitory factor (MIF) small interfering RNA (siRNA) in the presence of 400 μm methylglyoxal (MG) in human HaCaT keratinocytes. Cells were transfected with MIF siRNA or a control siRNA as well as recombinant human (rh)-MIF before stimulation with MG. Expression levels of MIF, glyoxalase I (GLO-I), and intraepidermal nerve fibers (IENF) mRNAs and proteins were measured by real-time reverse transcription polymerase chain reaction (a) to (c) and Western blot (d) to (g), respectively. Real-time PCR analysis was performed with a SYBR Green assay system. Relative gene expression levels normalized to β-actin was calculated with $2^{-\triangle\triangle CT}$ method. As a control for Western blot analysis, the level of β-actin was determined using an antibody against β-actin. All results are presented as mean ± SD of three independent experiments. $^{++}P< 0.01$, $^{+++}P<0.005$ compared to that in the group transfected with control siRNA.

that MIF can regulate GLO-I and IENF production under hyperglycemic skin conditions.

Discussion

Numerous studies have shown that chronic hyperglycemia is the main driving force of the development and progression of diabetic complication, including DN.[22–24] Increased glucose levels due to hyperglycemia can accelerate AGEs accumulation and damage the function of many proteins, including tubulin, mitochondrial electron transport chain proteins, insulin, and neuronal extracellular matrix proteins.[25,26] Several researches have shown that AGEs are elevated in peripheral nerves and skin of both diabetic patients and rodents.[27–29] Therefore, hyperglycemia can lead to

altered nerve conduction velocities, loss of epidermal innervation, and the onset of pain signs and symptoms in the feet.[27–29] Our results showed that DN rats had low body weights with excessive urination. They also developed mechanical sensitivity of the hind paw following STZ-induced hyperglycemic condition. GSH level was declined in footpad lesions of DN. Simultaneously, cell death was increased due to apoptosis and footpad thickness was thin. Normal skin tissue and cells have a steady rate of proliferation which is important for maintaining normal metabolism and structural integrity. Based on our results along with those of previous reports, when normal conditions undergo hyperglycemia, enhanced AGEs level might lead to dysfunctions of vital cellular processes by enhancing oxidative stress, resulting in loss of skin innervation which provokes pain.

It has been reported that AGEs produce neuronal damage and interact with cell surface receptors, particularly RAGE, to induce a cascade of intracellular signaling.[28] Activation of the pathway can lead to nuclear translocation of NF-kB[26,28] which is responsible for the expression of different classes of genes, including pro-inflammatory cytokines such as TNF-α and IL-6.[30] TRPV1, MRGPRD, or CGRP expressed on sensory neuron or transmembrane have multiple functions as cell sensors. They can mediate pain and inflammation.[31–34] We could not observe significant difference in expression levels of TRPV1, MRGPRD, CGRP, NF-kB, TNF-α, or IL-6 except for RAGE in footpad skin lesions of DN rats compared to those in sham rats. However, our results reveal that MIF expression levels were sharply and significantly up-regulated in footpad skin lesions of DN rats compared to those in sham rats. At the same time, expression levels of both GLO-I and IENF were significantly down-regulated in footpad skin lesions of DN rats compared to those in sham rats. Interestingly, MIF was mainly expressed in the basal layer of normal epidermis, showing colocalization with GLO-I. When normal conditions underwent hyperglycemia, MIF and GLO-I were reversely observed. In other words, MIF was overexpressed on the entire layer of the epidermis at large while GLO-I was faintly stained on the basal layer of the epidermis after induction of diabetes.

It has been reported that mechanical hypersensitivity induced by subcutaneous injection of rMIF into the hind paw of mice can be explained by local activation of nociceptors.[18,35,36] Many intracellular signaling and transcription factors triggered by rMIF also regulate pain states.[37,38] Thereby, MIF is likely to represent an important upstream mediator of factors contributing to pain. However, few studies have investigated the importance of MIF in DN.

Although the pathogenesis of DN is mainly due to the accumulation of a heterogeneous group of reactive sugars known as AGEs, the glyoxalase system can detoxify reactive dicarbonyls before they react with cellular components and form AGEs.[6,39,40] Several reports have shown that, in the peripheral nervous system, GLO-I is selectively expressed in small and unmyelinated peptidergic neurons and axons responsible for pain transmission.[7,41] Especially, GLO-I levels are known to be decreased after diabetes, subsequently exacerbating the pain of DN.[7,8]

The loss of cutaneous nerve fibers and behavioral measures have been used to assess the presence of sensory nerve damage characteristic of DN in both rodents and human patients.[3,4] Recently, several reports have reported that glycemic control is irrelevant to the onset of pain in DN patients who have survived type I diabetes.[9,10] Based on these previous reports, certain patients might have different mechanisms or parameters independent of glucose metabolism that allow them to remain pain free of DN.

To the best of our knowledge, this is the first study that characterizes the expression of MIF in the footpad of DN rats and to assess the contributory role of MIF to the pathogenesis of DN. Our results suggested that the development of pain was due to over-expression of MIF accompanied by low expression of GLO-I and IENF in the footpad of DN rather than due to neurotransmitters-activated inflammatory responses.

To determine whether MIF had any correlation with GLO-I and IENF in the footpad occurring pain signs of DN, we designed an in vitro model using keratinocytes of consistent with those obtained in footpad skins using DN rats. In our experiments, treatment of cells with rh-MIF under hyperglycemic condition sharply and significantly decreased expression levels of GLO-I and IENF compared to vehicle control treatment. Based on these results, it might be assumed that exogenous administration of MIF can competitively block enzymatic activity of GLO-I in the footpad of DN, thus suppressing the glyoxalase system and causing cellular impairment such as IENF. Intriguingly, siRNA-transfection caused knockdown of MIF gene in hyperglycemic keratinocytes increased expression levels of GLO-I and IENF in comparison with control siRNA-transfection, leading to recovery of GLO-I and IENF expression levels that were decreased by the induction of diabetes. Based on our results, MIF inhibition might allow GLO-I activities to be carried out smoothly to protect neurocellular innervation under DN, which may lead to pain relief.

We analyzed footpad skin tissues and cells where the pain would occur dominantly in DN. Examining the signaling transmission pathway of pain onset in DN is also important. Indeed, preliminary data from our lab indicated that MIF expression was increased in the footpad and spinal cord of DN rats. However, expression levels of inflammatory cytokines such as TNF-α, IL-1β, or IL-6 in footpad were not significantly changed, while those of spinal neurons were up-regulated considerably small in numbers compared to upregulation of MIF (unpublished data). Some reports have suggested that MIF can stimulate microglia and lead to inflammatory responses that enhance neuron excitability and provoke pain.[18,42,43] In light of these reports, further experiments are needed to analyze how MIF contributes to the extension of pain signal pathway in DN from the bottom of the footpad skin to the top of brain neurons. Based on previous reporting of GLO-I deficiency in neurons of DN,[7] we could not exclude possible correlations between MIF and GLO-I except for footpads considering DN pathophysiology.

Although we could not determine the exact pathogenesis of DN, our results suggest that MIF can aggravate

DN by suppressing GLO-I and IENF on the footpad and provoke pain. Also, it might be suggested that local administration of anti-MIF antibody can be potentially useful for diabetes patients who have excessive pain of footpad.

Taken together, it is suggested that MIF may offer a pharmacological approach to alleviate pain syndromes in DN.

Declaration of Conflicting Interests

Funding

ORCID iD

Sun Up Noh (iD) http://orcid.org/0000-0003-2091-8647

References

1. Boulton AJM, Vinik AI, Arezzo JC, Bril V, Feldman EL, Freeman R, Malik RA, Maser RE, Sosenko JM and Ziegler D. Diabetic neuropathies: a statement by the American Diabetes Association. *Diabetes Care* 2005; 28: 956–962.
2. Britland ST, Young RJ, Sharma AK and Clarke, BF. Association of painful and painless diabetic polyneuropathy with different patterns of nerve fiber degeneration and regeneration. *Diabetes* 1990; 39: 898–908.
3. Boric M, Skopljanac I, Ferhatovic L, Jelicic Kadic A, Banozic A and Puljak L. Reduced epidermal thickness, nerve degeneration and increased pain-related behavior in rats with diabetes type 1 and 2. *J Chem Neuroanat* 2013; 53: 33–40.
4. Lauria G, Lombardi R, Borgna M, Penza P, Bianchi R, Savino C, Canta A, Nicolini G, Marmiroli P and Cavaletti G. Intraepidermal nerve fiber density in rat foot pad: neuropathologic-neurophysiological correlation. *J Peripher Nerv Syst* 2005; 10: 202–208.
5. Chu CC, Wang SD, Chiang JS and Ho ST. Generalized depletion of free nerve endings and decrease of cutaneous nervous innervation in streptozotocin-induced painful and painless diabetic rats. *J Chin Med Assoc* 2012; 75: 314–321.
6. Jack MM and Wright DE. The role of advanced glycation endproducts and glyoxalase I in diabetic peripheral sensory neuropathy. *Transl Res* 2012; 159: 355–365.
7. Jack MM, Ryals JM and Wright DE. Characterization of glyoxalase I in streptozotocin-induced diabetic mouse models of painful and insensate neuropathy. *Diabetologia* 2011; 54: 2174–2182.
8. Jack MM, Ryals JM and Wright DE. Protection from diabetes-induced peripheral sensory neuropathy–a role for elevated glyoxasle I? *Exp Neurol* 2012; 234: 62–69.
9. Fullerton B, Jeitler K, Seitz M, Horvath K, Berghold A and Siebenhofer A. Intensive glucose control versus conventional glucose control for type 1 diabetes mellitus (review). *Cochrane Database Syst Rev* 2014; 2: CD009122.
10. Conway BN, Maynard JD and Orchard TJ. Protection from retinopathy and other complications in patients with type 1 diabetes of extreme duration: the joslin 50-year medalist study. *Diabetes Care* 2011; 34: 968–974.
11. Toso C, Emamaullee JA, Merani S and Shapiro AM. The role of macrophage migration inhibitory factor on glucose metabolism and diabetes. *Diabetologia* 2008; 51: 1937–1946.
12. Sanchez-Zamora Y, Terrazas LI, Vilches-Flores A, Leal E, Juárez I, Whitacre C, Kithcart A, Pruitt J, Sielecki T, Satoskar AR and Rodriguez-Sosa M. Macrophage migration inhibitory factor is a therapeutic target in treatment of non-insulin-dependent diabetes mellitus. *FASEB J* 2010; 24: 2583–2590.
13. Finucane OM, Reynolds CM, McGillicuddy FC, Harford KA, Morrison M, Baugh J and Roche HM. Macrophage migration inhibitory factor deficiency ameliorates high-fat diet induced insulin resistance in mice with reduced adipose inflammation and hepatic steatosis. *PLoS One* 2014; 9: e113369.
14. Atsumi T, Cho YR, Leng L, McDonald C, Yu T, Danton C, Hong EG, Mitchell RA, Metz C, Niwa H, Takeuchi J, Onodera S, Umino T, Yoshioka N, Koike T, Kim JK and Bucala R. The proinflammatory cytokine macrophage migration inhibitory factor regulates glucose metabolism during systemic inflammation. *J Immunol* 2007; 179: 5399–5406.
15. Calandra T, Bernhagen J, Metz CN, Spiegel LA, Bacher M, Donnelly T, Cerami A and Bucala R. MIF as a glucocorticoid-induced modulator of cytokine production. *Nature* 1995; 377: 68–71.
16. Noh SU and Park YM. The effect of green tea polyphenols on macrophage migration inhibitory factor-associated steroid resistance. *Br J Dermatol* 2012; 166: 653–657.
17. Calandra T and Roger T. Macrophage migration inhibitory factor: a regulator of innate immunity. *Nat Rev Immunol* 2003; 3: 791–800.
18. Alexander JK, Cox GM, Tian JB, Zha AM, Wei P, Kigerl KA, Reddy MK, Dagia NM, Sielecki T, Zhu MX, Satoskar AR, McTigue DM, Whitacre CC and Popovich PG. Macrophage migration inhibitory factor is essential for inflammatory and neuropathic pain and enhances pain in response to stress. *Exp Neurol* 2012; 236: 351–362.
19. Kleemann R, Mischke R, Kapurniotu A, Brunner H and Bernhagen J. Specific reduction of insulin disulfides by macrophage migration inhibitory factor with glutathione and dihydrolipoamide: potential role in cellular redox processes. *FEBS Lett* 1998; 430: 191–196.
20. Chaplan SR, Bach FW, Pogrel JW, Chung JM and Yaksh TL. Quantitative assessment of tactile allodynia in the rat paw. *J Neurosci Methods* 1994; 53: 55–63.

21. Rahman I, Kode A and Biswas SK. Assay for quantitative determination of glutathione and glutathione disulfide levels using enzymatic recycling method. *Nat Protoc* 2007; 1: 3159–3165.

22. Albers JW, Herman WH, Pop-Busui R, Feldman EL, Martin CL, Cleary PA, Waberski BH and Lachin JM. Effect of prior intensive insulin treatment during the Diabetes Control and Complication Trial (DCCT) on peripheral neuropathy in type 1 diabetes during the Epidemiology of Diabetes Interventions and Complications (EDIC) study. *Diabetes Care* 2010; 33: 1090–1096.

23. Tesfaye S, Stevens LK, Stephenson JM, Fuller JH, Plater M, Ionescu-Tirgoviste C, Nuber A, Pozza G and Ward JD. Prevalence of diabetic peripheral neuropathy and its relation to glycaemic control and potential risk factors: the EURODIAB IDDM Complications study. *Diabetologia* 1996; 39: 1377–1384.

24. Diabetes Control and Complications Trial Research Group, Nathan DM, Genuth S, Lachin J, Cleary P, Crofford O, Davis M, Rand L and Siebert C. The Diabetes Control and Complications Trial Research Group. The effect of intensive treatment of diabetes on the development and progression of long-term complications in insulin-dependent diabetes mellitus. *N Engl J Med* 1993; 329: 977–986.

25. Nass N, Bartling B, Navarrete Santos A, Scheubel RJ, Börgermann J, Silber RE and Simm A. Advanced glycation end products, diabetes and ageing. *Z Gerontol Geriatr* 2007; 40: 349–356.

26. Vincent AM, Perrone L, Sullivan KA, Backus C, Sastry AM, Lastoskie C and Feldman EL. Receptor for advanced glycation end products activation injures primary sensory neurons via oxidative stress. *Endocrinology* 2007; 148: 548–558.

27. Ahmed N, Babaei-Jadidi R, Howell SK, Beisswenger PJ and Thornalley PJ. Degradation products of proteins damaged by glycation, oxidation and nitration in clinical type 1 diabetes. *Diabetologia* 2005; 48: 1590–1603.

28. Lukic IK, Humpert PM, Nawroth PP and Bierhaus A. The RAGE pathway: activation and perpetuation in *the pathogenesis of diabetic neuropathy*. *Ann N Y Acad Sci* 2008; 1126: 76–80.

29. Meerwaldt R, Links TP, Graaff R, Hoogenberg K, Lefrandt JD, Baynes JW, Gans RO and Smit AJ. Increased accumulation of skin advanced glycation end-products precedes and correlates with clinical manifestation of diabetic neuropathy. *Diabetologia* 2005; 48: 1637–1644.

30. Bierhaus A, Haslbeck KM, Humpert PM, Liliensiek B, Dehmer T, Morcos M, Sayed AA, Andrassy M, Schiekofer S, Schneider JG, Schulz JB, Heuss D, Neundörfer B, Dierl S, Huber J, Tritschler H, Schmidt AM, Schwaninger M, Haering HU, Schleicher E, Kasper M, Stern DM, Arnold B and Nawroth PP. Loss of pain perception in diabetes is dependent on a receptor of the immunoglobulin superfamily. *J Clin Invest* 2004; 114: 1741–1751.

31. Gavva NR, Treanor JJ, Garami A, Fang L, Surapaneni S, Akrami A, Alvarez F, Bak A, Darling M, Gore A, Jang GR, Kesslak JP, Ni L, Norman MH, Palluconi G, Rose MJ, Salfi M, Tan E, Romanovsky AA, Banfield C and Davar G. Pharmacological blockade of the vanilloid receptor TRPV1 elicits marked hyperthermia in humans. *Pain* 2008; 136: 202–210.

32. Nilius B, Owsianik G, Voets T and Peters JA. Transient receptor potential cation channels in disease. *Physiol Rev* 2007; 87: 165–217.

33. Megan SJ, Janelle MR and Douglas EW. Early loss of peptidergic intraepidermal nerve fibers in an STZ-induced mouse model of insensate diabetic neuropathy. *Pain* 2008; 140: 35–47.

34. Cavanaugh DJ, Lee H, Lo L, Shields SD, Zylka MJ, Basbaum AI and Anderson DJ. Distinct subsets of unmyelinated primary sensory fibers mediate behavioral responses to noxious thermal and mechanical stimuli. *Proc Natl Acad Sci USA* 2009; 106: 9075–9080.

35. Wang F, Shen X, Guo X, Peng Y, Liu Y, Xu S and Yang J. Spinal macrophage migration inhibitory factor contributes to the pathogenesis of inflammatory hyperalgesia in rats. *Pain* 2010; 148: 275–283.

36. Wang F, Xu S, Shen X, Guo X, Peng Y and Yang J. Spinal macrophage migration inhibitory factor is a major contributor to rodent neuropathic pain-like hypersensitivity. *Anesthesiology* 2011; 114: 643–659.

37. Mitchell RA, Metz CN, Peng T and Bucala R. Sustained mitogen-activated protein kinase (MAPK) and cytoplasmic phospholipase A1 activation by macrophage migration inhibitory factor (MIF). Regulatory role in cell proliferation and glucocorticoid action. *J Biol Chem* 1999; 274: 18100–18106.

38. Wang F, Wu H, Xu S, Guo X, Yang J and Shen X. Macrophage migration inhibitory factor activates cyclooxygenase 2-prostaglandin E(2) in cultured spinal microglia. *Neurosci Res* 2011; 71: 210–218.

39. Brouwers O, Niessen PM, Ferreira I, Miyata T, Scheffer PG, Teerlink T, Schrauwen P, Brownlee M, Stehouwer CD and Schalkwijk CG. Overexpression of glyoxalase-I reduces hyperglycemia-induced levels of advanced glycation endproducts and oxidative stress in diabetic rats. *J Biol Chem* 2011; 286: 1374–1380.

40. Rabbani N and Thornalley PJ. Glyoxalase in diabetes, obesity and related disorders. *Semin Cell Dev Biol* 2011; 22: 309–317.

41. Sabrina R, Emmanuelle L, Sylvianne S, Carine N, Bertrand F and Isabelle P. Skin protection against dicarbonyl stress by the glyoxalase system. *Free Radic Biol Med* 2014; 75: s18–s20.

42. Cox GM, Kithcart AP, Pitt D, Guan Z, Alexander J, Williams JL, Shawler T, Dagia NM, Popovich PG, Satoskar AR and Whitacre CC. Macrophage migration inhibitory factor potentiates autoimmune-mediated neuroinflammation. *J Immunol* 2013; 191: 1043–1054.

43. Bay-Richter C, Janelidze S, Sauro A, Bucala R, Lipton J, Deierborg T and Brundin L. Behavioural and neurobiological consequences of macrophage migration inhibitory factor gene deletion in mice. *J Neuroinflammation* 2015; 12: 163–173.